Appl Phys B (2010) 99: 67–74
DOI 10.1007/s00340-009-3817-0

Applied Physics B
Lasers and Optics

Circularly polarized localized near-field radiation at the nanoscale

E. Öğüt · G. Kızıltaş · K. Şendur

Received: 27 August 2009 / Revised version: 22 October 2009 / Published online: 14 November 2009

Abstract Diffraction-limited circularly polarized electromagnetic radiation has been widely used in the literature for various applications at both optical and microwave frequencies. With advances in nanotechnology, emerging plasmonic nano-optical applications, such as all-optical magnetic recording, require circularly polarized electromagnetic radiation beyond the diffraction limit. In this study, a plasmonic cross-dipole nano-antenna is investigated to obtain a circularly polarized near-field optical spot with a size smaller than the diffraction limit of light. A cross-dipole nano-antenna is composed of four metallic nano-rods placed at a perpendicular orientation with respect to each other. The performance of the nano-antenna is investigated through numerical simulations. In the first part of this study, the nano-antenna is illuminated with a diffraction-limited circularly polarized radiation. An optimal antenna geometry is specified to obtain an intense optical spot that satisfies two necessary conditions for circular polarization: a phase difference of 90° and a unit amplitude ratio between the electric field components in the vicinity of the antenna gap. In the second part of this study, the nano-antenna is illuminated with diffraction-limited linearly polarized radiation. It is shown that the phase difference between the electric field components can be adjusted by selecting either different antenna lengths or different gap distances in the vertical and horizontal directions. Due to the relatively short wavelength of surface plasma waves on the antenna, it is demonstrated that the phase difference can be sufficient to obtain circularly polarized light. An optimal physical configuration for the nano-antenna and the polarization angle of the incident light is identified to obtain a circularly polarized optical spot beyond the diffraction limit from diffraction-limited linearly polarized radiation.

E. Öğüt · G. Kızıltaş · K. Şendur (✉)
Faculty of Engineering and Natural Sciences, Sabancı University, Orhanlı–Tuzla, Istanbul 34956, Turkey
e-mail: sendur@sabanciuniv.edu

1 Introduction

Circular polarization is utilized in various applications at radio frequency and microwave regimes due to its advantages, such as increased efficiency in power transmission. In satellite communications [1], for example, the polarization angle of a linearly polarized electromagnetic wave is tilted due to the anisotropy of the ionosphere [1]. A mismatch between the polarization angle of the incident radiation and receiving antenna causes a loss of transmitted power. Circularly polarized radiation, however, is less sensitive to ionospheric rotation. Therefore, utilizing a circularly polarized transmitting and receiving antenna pair results in increased transmitted power.

At optical frequencies, circular polarization promises to be a rotary power source for various applications. One potential application utilizes circularly polarized light to probe nuclear moments by creating electron spins in semiconductors [2]. In another application, microgears are rotated by circularly polarized light [3]. Low threshold laser action of dye-doped cholesteric liquid crystals is demonstrated using input circularly polarized light [4]. In addition to the aforementioned applications, circularly polarized light may also be utilized to probe a medium. By utilizing circularly polarized laser light, the response of a single chiral molecule is probed [5] and optically active single-walled carbon nanotubes are characterized by circular dichroism spectroscopy, which uses circularly polarized light [6]. In a recent study,

a plasmonic polarizer is utilized to obtain a far-field circular polarization [7]. The plasmonic polarizer is composed of two aperture grating structures perpendicular to each other and carrying two linearly polarized collimated beams with equal amplitudes. All of the aforementioned applications utilize diffraction-limited circularly polarized electromagnetic radiation, which is sufficient to fulfill the requirements of those applications.

With advances in nanotechnology, circularly polarized electromagnetic radiation beyond the diffraction limit is desired in emerging plasmonic nano-applications. One of these applications is all-optical magnetic recording [8, 9]. Stanciu et al. [8, 9] demonstrated that magnetization can be reversed in a reproducible manner by using a circularly polarized optical beam without any externally applied magnetic field. The size of the magnetization reversal in that study was on the order of 20 microns due to the large optical spots that were utilized. To advance the areal density of hard disk drives beyond 1 Tbit/in.^{2}, magnetization reversal areas much smaller than 100 nm are required. To achieve sub-100 nm bits in an all-optical magnetic recording system, a circularly polarized optical spot beyond the diffraction limit is necessary.

In this study, two different schemes are investigated to obtain a circularly polarized optical spot with dimensions smaller than the diffraction-limit. In Sect. 2, a cross-dipole nano-antenna is introduced to obtain a circularly polarized optical spot with a size beyond the diffraction limit when the antenna is illuminated with diffraction-limited circularly polarized radiation. An optimal antenna geometry is specified to obtain an intense optical spot that satisfies two necessary conditions for circular polarization: a phase difference of 90° and a unit amplitude ratio between the electric field components in the vicinity of the antenna gap. In Sect. 3, we demonstrate that the phase difference between the electric field components can be adjusted by selecting either different antenna lengths or gap distances in the vertical and horizontal directions. Since the plasma wavelengths on the antenna are much shorter than the wavelength of incident radiation, a circularly polarized optical spot beyond the diffraction limit is obtained from diffraction-limited linearly polarized incident radiation. Concluding remarks appear in Sect. 4.

2 Circularly polarized illumination using a cross-dipole nano-antenna

Optical antennas have a long history and there are many experimental studies in the literature including early optical rectification works [10–12] and more recent resonant antennas [13–16]. Nano-antennas [17–20] have been utilized in existing and emerging nano-optical applications, such as scanning near-field optical microscopy [21], data storage [22], nano-lithography [23], and biochemical sensing [24]. Three main features of the antennas have been attractive for existing and emerging applications: their ability to obtain optical spots beyond the diffraction limit, their potential to achieve higher power transmittance to the sample, and a narrow and adjustable spectral response.

Although their ability to achieve these three goals has attracted a significant amount of interest, their ability to obtain light with various polarizations has attracted little attention. Ohdaira et al. [25] obtained local circular polarization by superposing two cross-propagating evanescent waves. In this study, we suggest an alternative technique to obtain intense localized circular polarization with a plasmonic nano-antenna. The nano-antennas in the literature obtained optical spots beyond the diffraction limit with linear polarization. However, there are emerging nanotechnology applications, such as all-optical magnetic recording [8, 9], that require circularly polarized light beyond the diffraction limit. To address this emerging need, it is desirable to obtain optical spots with circular polarization.

In this study, a metallic cross-dipole antenna is suggested to obtain a circularly polarized optical spot with a size beyond the diffraction limit. A cross-dipole antenna, which is shown in Fig. 1, is composed of four metallic nano-rods placed at a perpendicular orientation with respect to each other. The geometric parameters are identified in Fig. 1. The antenna particles have equal horizontal and vertical lengths $L_h = L_v$ and are separated from each other by a distance $G_v = G_h$ in both vertical and horizontal directions. To obtain circular polarization from linearly polarized incident

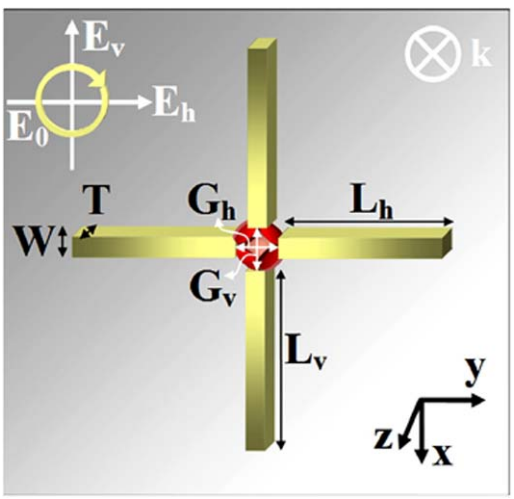

Fig. 1 Schematic illustration of the cross-dipole antenna. The incident electric field **E** has a clockwise orientation, which propagates along the **k**-vector. L_h and L_v are the lengths of the horizontal and vertical antenna particles, and G_h and G_v are the gap distances of the horizontal and vertical antenna particles. T is the thickness and W is the width of the antenna particles

light, these conditions will be relaxed in Sect. 3 and antennas with different lengths and gap distances will also be used. The length of each antenna particle is $L = 130$ nm, the width is $W = 10$ nm, and the particle thickness is $T = 20$ nm. The center of the antenna is located at the origin, therefore, it lies between $z = -10$ nm and $z = 10$ nm. The antenna is surrounded by vacuum. Based on a previous study [26] on nano-antennas, the operating wavelength is selected as $\lambda = 1100$ nm. The dielectric constant of gold at $\lambda = 1100$ nm is selected as $\epsilon_{\text{gold}} = -58.8971 - j4.61164$ [27]. The amplitude of the incident radiation is selected as 1 V/m, therefore, the electric field values reported in this study correspond to the field enhancement of the antenna. Incident circularly polarized radiation propagates in the negative $\hat{z}$-direction.

Figure 2 illustrates the intensity distributions for a cross-dipole antenna when it is illuminated with a diffraction-limited circularly polarized light at $\lambda = 1100$ nm. Projection of the cross-dipole antenna boundaries (thin white contour) is added to the figure to illustrate the relative position of the optical spot with respect to the antenna. In Fig. 2(a) the intensity distribution is presented at the $z = 0$ nm, which passes through the center of the antenna. The results in Fig. 2(a) suggest that the cross-dipole antenna achieves a localized intense spot in the gap region of the antenna. In Fig. 2(b), intensity distribution on the $z = 20$ nm is illustrated. This plane is located at a distance of 10 nm below the bottom surface of the antenna, therefore, it represents a typical intensity distribution at the sample plane. Since a tightly confined optical spot diverges quickly in relatively short distances [28], a broader optical spot is observed in Fig. 2(b) as compared to Fig. 2(a). As the observation plane is placed further away from the antenna, the intensity obtained by the antenna gets smaller and the spot size increases. The reduction of the field intensity is due to the sharp decay of evanescent fields away from the nano-antenna.

The incident circularly polarized diffraction-limited radiation can be decomposed into two components: a horizontal and a vertical component of equal amplitude with a 90° phase difference between them. Each of these components creates an induced current along their respective axes on the antenna. These induced currents are the source of charge accumulation at the ends of the antenna. The charges created across the gap separating the metallic parts of the antenna have opposite polarity. The oscillation of the charges in the horizontal and vertical directions is the source of the localized near-field electromagnetic radiation.

Although the fundamentals of the optical energy localization for the cross-dipole antenna are similar to that of a simple dipole antenna, additional factors complicate the interaction of the circularly polarized incident light and nano-antenna. The charge accumulation at the end of a horizontal-oriented particle interacts not only with the other horizontal-oriented particle but also with the vertical-oriented particles. Although the interaction between the horizontal and vertical-oriented dipole is strong as seen in Fig. 2(a), the contribution of these dipoles has less of an impact on the field distribution at the sample plane as shown in Fig. 2(b). The near-field radiation due to the interaction between a horizontal and a vertical particle is more localized since it is mainly concentrated around the corners due to the lightning-rod effect. Although near-field radiation around a corner is quite strong at the source plane as seen in Fig. 2(a), it also has a faster decay rate than the broader near-field dipole radiation. Therefore, its impact is less pronounced at the sample plane as shown in Fig. 2(b). The optical spot, however, slightly broadens due to this effect.

To obtain circular polarization within the localized optical spot, two additional requirements need to be met: a phase difference of 90° and a unit amplitude ratio between the x- and y-oriented electric field components in the vicinity of the antenna gap. Due to the symmetry of the geometry in perpendicular directions, a 90° phase difference is obtained in the gap region of the antenna as shown in Fig. 3(a). Since our aim is to obtain a circularly polarized optical spot, the 90° phase difference requirement needs to be satisfied only within the optical spot in the gap region.

As shown in Fig. 3(b), the relative amplitude of the horizontal and vertical field is the same within the optical spot

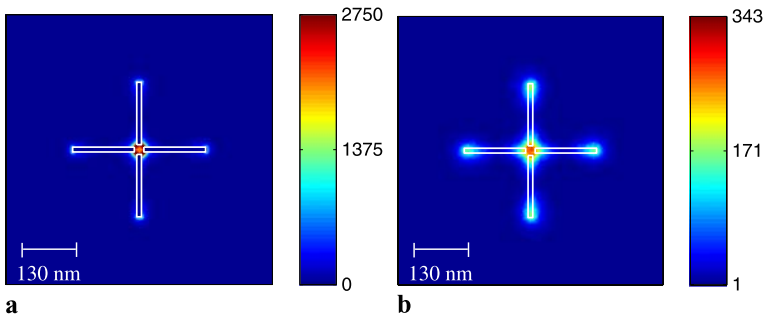

Fig. 2 Intensity distributions for a cross-dipole antenna on $z = 0$ and $z = 20$ nm when the antenna is illuminated with a diffraction-limited circularly polarized light: (**a**) $|\mathbf{E}(x, y, z = 0)|^2$ and (**b**) $|\mathbf{E}(x, y, z = 20)|^2$. Projection of the cross-dipole antenna boundaries (*thin white contour*) is added to the figure to illustrate the relative position of the optical spot with respect to the antenna

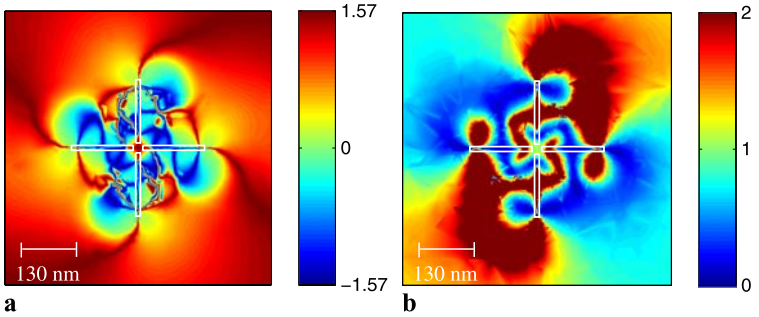

Fig. 3 (**a**) Phase difference $|\Delta\phi(x, y, z = 20)|$ and (**b**) Electric field intensity ratio $|\mathbf{E_y}(x, y, z = 20)|/|\mathbf{E_x}(x, y, z = 20)|$ for circularly polarized incident light. Dimensions are selected as $L = 130$ nm, $G = 20$ nm, $W = 10$ nm, $T = 20$ nm and $\lambda = 1100$ nm. Projection of the cross-dipole antenna boundaries (*thin white contour*) is added to the figure to illustrate the relative position of the optical spot with respect to the antenna

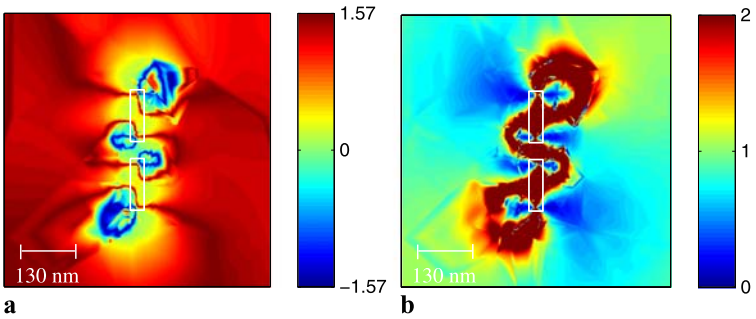

Fig. 4 (**a**) $|\Delta\phi(x, y, z = 20)|$ and (**b**) $|\mathbf{E_y}(x, y, z = 20)|/|\mathbf{E_x}(x, y, z = 20)|$ for circularly polarized incident light. Dimensions are selected as $L = 70$ nm, $G = 23$ nm, $W = 19$ nm, $T = 20$ nm and $\lambda = 700$ nm

due to the symmetry of the geometry. Therefore, the unit amplitude ratio requirement between the horizontal and vertical components is satisfied within the optical spot. The results in Fig. 3 suggest that all three conditions, i.e. localized radiation with intense amplitude, phase difference, and relative amplitude between components, are only satisfied in the optical spot defined by the gap region of the cross-dipole nano-antenna. As illustrated in Figs. 2 and 3, all three conditions are met within the optical spot, therefore, a circularly-polarized localized optical spot is obtained. The sense of circular polarization is right-handed, since the electric field **k**-vector is directed along the negative z-direction and the circularly polarized light is clockwise oriented.

The particles of a cross-dipole antenna are perpendicular with respect to each other, therefore, the cross-dipole geometry supports field components that are perpendicular to each other. Circularly polarized radiation has both horizontal and vertical polarized electric field components, which have a phase difference of 90°. Since a simple dipole antenna has particles only along one orientation, circular polarization cannot be obtained by a dipole antenna that is composed of only horizontally or vertically aligned nanoparticles. In Fig. 4, the results of a vertical dipole antenna are illustrated. Figure 4(a) and (b) shows the phase difference and relative amplitude for a vertical dipole antenna illuminated with diffraction-limited circularly polarized light. As the results suggest, the conditions are not met for circular polarization. The dipole antenna only responds to the vertical component of the incident light, therefore, the localized near-field radiation is linearly polarized. A vertical dipole antenna acts as a combination of a nano-lens and a vertical-oriented polarizer when it is illuminated with a circularly polarized radiation.

In the numerical simulations in this work, the performance of the nano-antenna is considered in free space. When the nano-antennas are manufactured on glass using lithographic techniques, it is expected that the resonance wavelength will shift toward longer wavelengths since resonance of nano-particles placed on a dense medium redshifts [29].

3 Obtaining circularly polarized optical spots from a linearly polarized diffraction-limited illumination

Circular polarization can be decomposed into a horizontal and a vertical component. Similarly, any linear polarization can also be decomposed into a horizontal and a vertical component. One of the main differences between linear and circular polarization is the phase difference between the perpendicular components. The phase difference between the perpendicular components for linear polarization is 0°, whereas for circular polarization the difference is 90°. The phase difference is not the only difference between linear

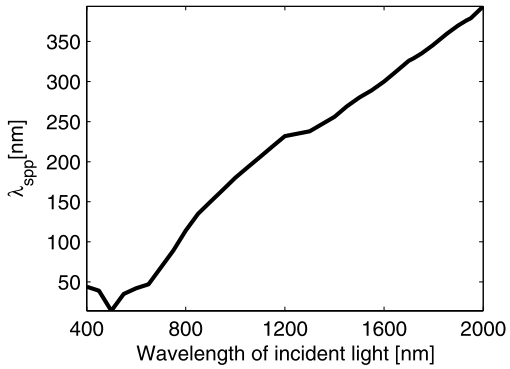

Fig. 5 Wavelength of plasma wave on the antenna versus the wavelength of incident light

and circular polarization. The amplitude ratio for the horizontal and vertical components is unity in circular polarization, whereas there is no such requirement for linear polarization.

Based on the aforementioned differences, there are three challenges for producing a circularly polarized optical spot beyond the diffraction limit from a linearly polarized diffraction-limited incident radiation: (1) focusing the incident light into an optical spot beyond the diffraction limit, (2) producing a 90° phase difference at the output radiation from an incident radiation that has a 0° phase difference, and (3) obtaining horizontal and vertical components with equal amplitudes. Focusing the incident light into a small optical spot will be achieved by the cross-dipole nano-antenna. To obtain a nonzero phase difference and a unit perpendicular amplitude ratio, the cross-dipole nano-antenna will be modified.

The phase difference between perpendicular components is obtained by using the short plasma wavelength of plasmonic nano-antennas. The relation between the plasma wavelength and antenna geometry has been investigated recently by an analytical treatment [20] and a finite element based solution [26]. The results suggested that for plasma metals, such as gold which is used in this study, the plasma wavelength over the nano-antenna is much shorter than the wavelength of the incident photon. For example, the effective plasma wavelength over a gold nanoparticle is plotted as a function of the wavelength of incident light in Fig. 5. The width of the gold nanoparticle is 10 nm. As shown in Fig. 5, the plasma wavelength is on the order of 200 nm when the wavelength of incident beam is 1100 nm. Such short effective plasma wavelengths of thin nanoparticles will be utilized to produce the desired phase difference between the horizontal and vertical components.

The phase of the waves on the horizontal-oriented particles and the horizontal location x around the antenna are related as

$$\phi_H = \phi_H^{\text{inc}} + 2\pi x/\lambda_{\text{spp}} \tag{1}$$

where ϕ_H^{inc} is the phase of the horizontal component of the incident beam and λ_{spp} is the plasma wavelength. Similarly, the phase of the waves on the vertical-oriented particles and the vertical location y around the antenna are related as

$$\phi_V = \phi_V^{\text{inc}} + 2\pi y/\lambda_{\text{spp}} \tag{2}$$

where ϕ_V^{inc} is the phase of the vertical component of the incident beam. The phase difference between the horizontal and vertical components of the near-field radiation around the center of the antenna is given as

$$\Delta\phi = \phi_H - \phi_V = \left(\phi_H^{\text{inc}} - \phi_V^{\text{inc}}\right) + 2\pi(x-y)/\lambda_{\text{spp}} \tag{3}$$

which will yield a phase difference

$$\Delta\phi = \left(\phi_H^{\text{inc}} - \phi_V^{\text{inc}}\right) \tag{4}$$

at the center of the gap since $x = y = 0$. For example, the phase difference between the horizontal and vertical components of the output near-field radiation is obtained as $\Delta\phi = 0°$ for a linearly polarized incident beam since $\phi_H^{\text{inc}} - \phi_V^{\text{inc}} = 0°$. Similarly, we obtain $\Delta\phi = 90°$ for a circularly polarized incident beam. These expectations are in agreement with the results in Sect. 2.

Since linearly polarized incident radiation has a $(\phi_H^{\text{inc}} - \phi_V^{\text{inc}}) = 0°$ phase difference and $x - y = 0$ at the center of the antenna, an additional phase term is necessary in (3) to convert a linearly polarized incident beam to a circularly polarized output. Producing the desired phase difference can be accomplished by creating an asymmetry in the antenna geometry. In this study, an additional phase term is introduced into (3) by either (1) using a slightly different antenna length for the horizontal-oriented antenna L_h and vertical-oriented antenna L_v, or (2) using a different horizontal gap distance G_h and a vertical gap distance G_v for the cross-dipole antenna. With slightly different antenna lengths, the phase of the near-field radiation around the center of the antenna is given as

$$\Delta\phi = \phi_H - \phi_V = \left(\phi_H^{\text{inc}} - \phi_V^{\text{inc}}\right) + 2\pi(x-y) /\lambda_{\text{spp}} + 2\pi(L_h - L_v)/\lambda_{\text{spp}} \tag{5}$$

which will yield at the center of the gap

$$\Delta\phi = \left(\phi_H^{\text{inc}} - \phi_V^{\text{inc}}\right) + 2\pi(L_h - L_v)/\lambda_{\text{spp}} \tag{6}$$

Therefore, to obtain a $\Delta\phi = 90°$, the horizontal and vertical antenna lengths should satisfy

$$2\pi(L_h - L_v)/\lambda_{\text{spp}} = \pi/2 \tag{7}$$

which yields

$$L_h - L_v = \lambda_{\text{spp}}/4 \tag{8}$$

When the difference between the length of the particles $L_h - L_v$ is set to $\lambda_{spp}/4$, the desired phase difference at the output radiation can be achieved. As discussed before and as illustrated in Fig. 5, the effective wavelengths for the plasma waves on the nano-antenna are much shorter than the wavelength of light. For example, when the incident wavelength is 700 nm, the quarter of the effective plasma wavelength corresponds to $\lambda_{spp}/4 = 17$ nm for an antenna with a thickness of 10 nm. Similarly, an operating wavelength of 1100 nm corresponds to $\lambda_{spp}/4 = 50$ nm. Such small $\lambda_{spp}/4$ values enable us to obtain a phase difference by using different L_h and L_v values without a significant decay of the horizontal or vertical near-field radiation amplitude.

The amplitude of the near-field radiation depends on the antenna length and the gap distance. Changing the symmetry of the antenna by using different (L_h, L_v) or (G_h, G_v) values will impact the amplitude of the horizontal and vertical components. The decay of the amplitude of the vertical (or horizontal) field component needs to be compensated to achieve a circular polarization, which requires these components to be equal. Any decay of the output field amplitudes can be compensated by adjusting the polarization angle of the incident linearly polarized wave, as shown in Fig. 6. If the amplitude of the vertical field component is small due to the created asymmetry, the polarization angle α_{pol} needs to be increased to achieve circular polarization.

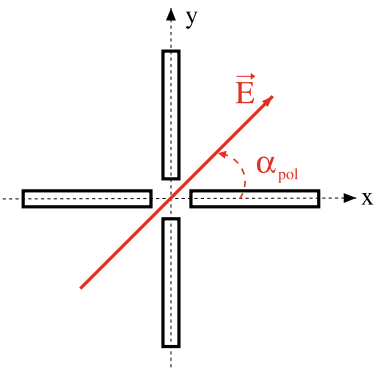

Fig. 6 Illustration of the top view of the cross-dipole antenna. The polarization angle of the linearly polarized incident field is shown with respect to the antenna orientation

The effect of $L_h - L_v$ on $\Delta\phi$ and $|\mathbf{E_y}|/|\mathbf{E_x}|$ is illustrated in Fig. 7. The cross-dipole is illuminated with a linearly polarized incident field with a polarization angle of $\alpha_{pol} = 45°$. The wavelength is $\lambda = 1100$ nm. In Fig. 7 we plot various L_v as a function of electric field amplitude E, phase difference $\Delta\phi$, and electric field amplitude ratio E_y/E_x at the point $x = 0$, $y = 0$, $z = 20$ nm. The results in Fig. 7(a) indicate that a phase difference, $\Delta\phi(x = 0, y = 0, z = 20\text{ nm}) \neq 0$, is obtained by creating an asymmetry between L_h and L_v. The results in Fig. 7(a) suggest that at $L_v = 160$ nm we obtain $E = 12.6$ V/m, $\Delta\phi = -1.57$ rad and $E_y/E_x = 0.31$. As L_v decreases to 130 nm, $\Delta\phi$ decreases to 0 rad, since the cross-dipole becomes symmetric and the phase difference due to $L_v - L_h$ in (5) vanishes. The results suggest that by operating the nano-antenna at 1100 nm, an elliptically polarized near-field radiation is obtained for L_v values between 130 and 160 nm. When L_v is exactly 130 nm, the localized radiation becomes linearly polarized.

The strong near-field radiation is also preserved in Fig. 7(b), while obtaining a phase difference $\Delta\phi \neq 0°$. The result in Fig. 7(b) suggests that the cross-dipole antenna creates a strong near-field radiation when L_v is in the 130–160 nm range. As shown in Fig. 7(b), E has a strong value at 130 nm when the antenna is symmetric. Although the antenna loses its radiation strength, the near-field radiation is still strong in the 130–160 nm range.

In Fig. 8, electric field intensity $|E|^2$, $\Delta\phi$, and E_y/E_x are plotted on the $z = 20$ nm for $L_v = 160$ nm and $L_h = 130$ nm. As shown in Fig. 8(b), $\Delta\phi$ value of -1.57 rad is achieved at $L_v = 160$ nm. However, a $\Delta\phi$ value of -1.57 rad is not sufficient. The E_y/E_x ratio should be unity. To reach a circular polarization, E_y/E_x needs to be further increased. One way to achieve this is to change the polarization angle of the incident radiation. As shown in Fig. 9, the E_y/E_x ratio is increased from 0.31 to 1 by changing the polarization angle α_{pol} of the incident linear radiation from 45° to 72°. As shown in Fig. 9, as the polarization angle is increased to $\alpha_{pol} = 72°$, $\Delta\phi$ keeps constant around -1.57, while E_y decreases to 7.3 V/m. Figure 10(a) results in a localized region of intense electric field distribution. Figure 10(b) and (c) represents the localization of phase difference and amplitude ratio between

Fig. 7 Effect of various L_v values on (**a**) $|\Delta\phi(x = 0, y = 0, z = 20)|$ and $|\mathbf{E_y}(x = 0, y = 0, z = 20)|/|\mathbf{E_x}(x = 0, y = 0, z = 20)|$, (**b**) $|\mathbf{E}(x = 0, y = 0, z = 20)|$. Dimensions selected as $G_h = G_v = 20$ nm, $L_h = 130$ nm, $T = 20$ nm, $W = 10$ nm and $\lambda = 1100$ nm

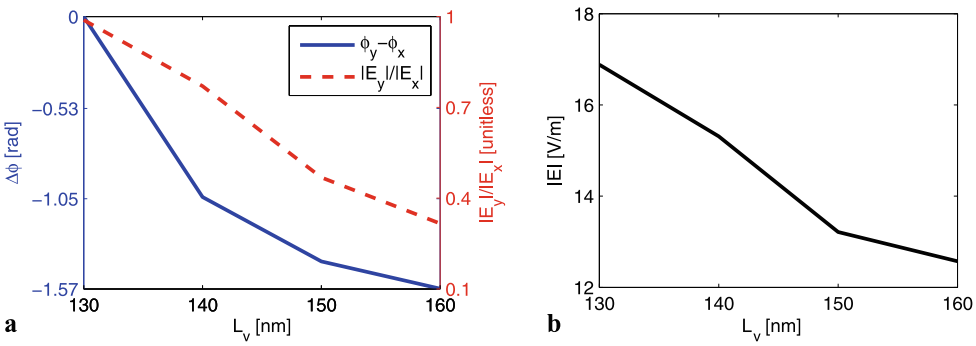

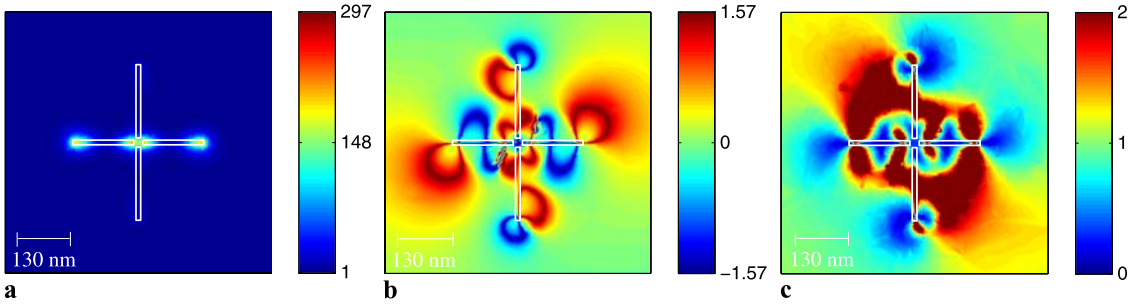

Fig. 8 (**a**) $|\mathbf{E}(x, y, z = 20)|^2$, (**b**) $|\Delta\phi(x, y, z = 20)|$ and (**c**) $|\mathbf{E_y}(x, y, z = 20)|/|\mathbf{E_x}(x, y, z = 20)|$ for $\alpha_{\text{pol}} = 45°$. Dimensions are selected as $L_v = 160$ nm and $L_h = 130$ nm

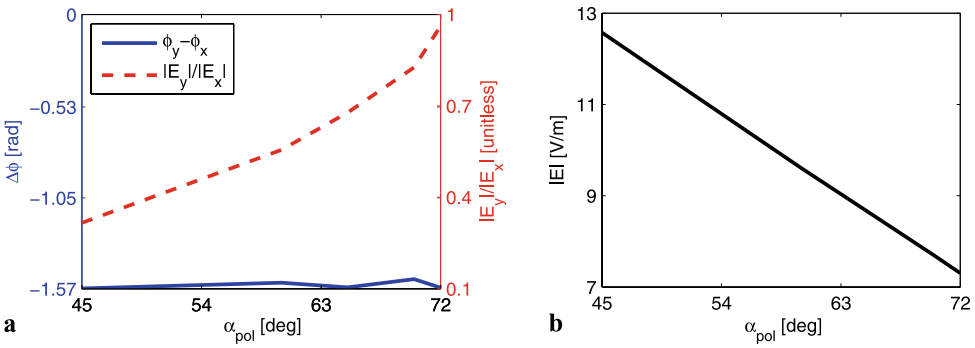

Fig. 9 Effect of various α_{pol} values on (**a**) $|\Delta\phi(x = 0, y = 0, z = 20)|$ and $|\mathbf{E_y}(x = 0, y = 0, z = 20)|/|\mathbf{E_x}(x = 0, y = 0, z = 20)|$ and (**b**) $|\mathbf{E}(x = 0, y = 0, z = 20)|^2$. Dimensions are selected as $L_v = 160$ nm, $L_h = 130$ nm, $G_h = 20$ nm, $G_v = 20$ nm, $T = 20$ nm, $W = 10$ nm and $\lambda = 1100$ nm

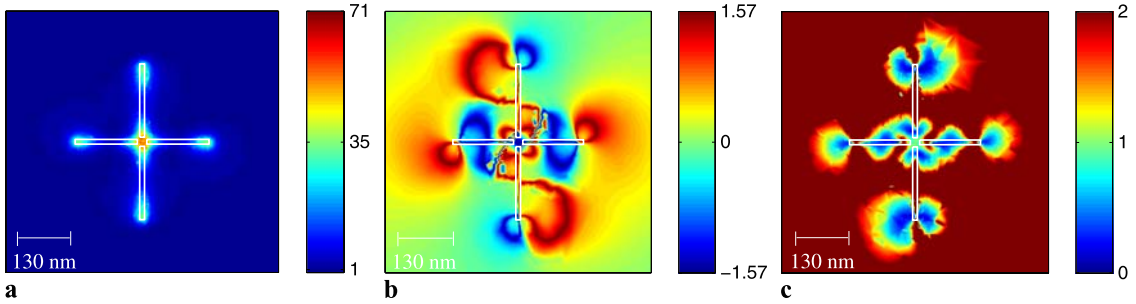

Fig. 10 (**a**) $|\mathbf{E}(x, y, z = 20)|^2$, (**b**) $|\Delta\phi(x, y, z = 20)|$ and (**c**) $|\mathbf{E_y}(x, y, z = 20)|/|\mathbf{E_x}(x, y, z = 20)|$ for $\alpha_{\text{pol}} = 72°$. Dimensions are selected as $L_v = 160$ nm and $L_h = 130$ nm

the field components. The phase difference is confined in a small space with dimensions beyond the diffraction limit and with a value around -1.57 rad. The amplitude ratio is also confined in a small space with a value around 1. Therefore, the result in Fig. 10(b) and (c) indicates that a circularly polarized region of space is obtained at $z = 20$ nm. The sense of circular polarization is left-handed, since the electric field **k**-vector is directed along the negative z direction, the circularly polarized light is counterclockwise oriented.

As mentioned previously, another way to introduce a phase difference in (5) is to introduce a gap difference $G_h - G_v$, rather than antenna length difference $L_h - L_v$. A sample result for obtaining a phase difference using $G_h - G_v$ is illustrated in Fig. 11. As shown in Fig. 11, for $G_h - G_v = 44$ nm, $\Delta\phi$ is equal to 1.57 rad and E_y/E_x possesses a unity value at $z = 20$ nm.

4 Conclusion

In this study, a near-field localized region of circularly polarized light beyond the diffraction limit is achieved using a cross-dipole optical antenna. It was demonstrated that a cross-dipole nano-antenna with a symmetric structure can convert diffraction-limited circularly polarized radiation into a circularly polarized optical spot well-beyond the diffraction limit. It was also shown that a phase difference can be obtained between field components by utilizing an asymmetric cross-dipole nano-antenna. It was shown that a phase

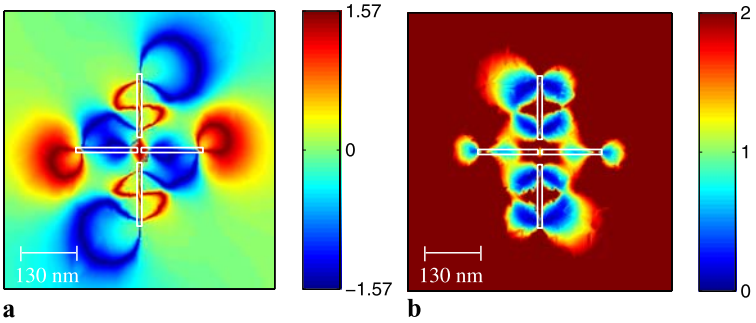

Fig. 11 (**a**) $|\Delta\phi(x, y, z = 20)|$ and (**b**) $|\mathbf{E_y}(x, y, z = 20)|/|\mathbf{E_x}(x, y, z = 20)|$ for linearly polarized incident light with $\alpha_{\text{pol}} = 73°$. Dimensions are selected as $L = 130$ nm, $G_h = 8$ nm, $G_v = 52$, $W = 10$ nm, $T = 20$ nm and $\lambda = 1100$ nm

difference between the electric field components can be adjusted by selecting either different antenna lengths or different gap distances in the vertical and horizontal directions. Our results indicate that it is feasible to convert linearly polarized diffraction-limited radiation into a circularly polarized optical spot well beyond the diffraction limit due to the short wavelength of surface plasma waves on the antenna. An optimal physical configuration for the nano-antenna and the polarization angle of the incident light was identified to obtain a circularly polarized optical spot beyond the diffraction limit from diffraction-limited linearly polarized radiation.

Acknowledgements This work was performed with the support of the European Community Marie Curie International Reintegration Grant (IRG) Agreement Number MIRG-CT-2007-203690.

References

1. J. Volakis, *Antenna Engineering Handbook* (McGraw-Hill, New York, 2007)
2. J.M. Kikkawa, D.D. Awschalom, Science **287**, 473 (2000)
3. S. Neale, M. Macdonald, K. Dholakia, T.F. Krauss, Nature **4**, 530 (2005)
4. Y. Matsuhisa, Y. Huang, Y. Zhou, S.T. Whu, Opt. Express **15**, 622 (2007)
5. R. Hassey, E.J. Swain, N.I. Hammer, D. Venkataraman, M.D. Barnes, Science **314**, 1437 (2006)
6. X. Peng, N. Komatsu, S. Bhattacharya, T. Shimawaki, S. Aonuma, T. Kimura, A. Osuka, Nature **2**, 361 (2007)
7. N. Yu, Q.Y. Wang, C. Pflügl, L. Diehl, F. Capasso, T. Edamura, S. Furuta, M. Yamanishi, H. Kan, Appl. Phys. Lett. **94**, 151101 (2009)
8. C.D. Stanciu, F. Hansteen, A.V. Kimel, A. Kirilyuk, A. Tsukamoto, A. Itoh, Th. Rasing, Phys. Rev. Lett. **99**, 047601 (2007)
9. J. Hohlfeld, C.D. Stanciu, A. Rebei, Appl. Phys. Lett. **94**, 152504 (2009)
10. S. Wang, Appl. Phys. Lett. **28**, 303 (1976)
11. V. Daneu, D. Sokoloff, A. Sanchez, A. Javan, Appl. Phys. Lett. **15**, 398 (1969)
12. A. Sanchez, C.F. Davis, Jr., K.C. Liu, A. Javan, J. Appl. Phys. **49**, 5270 (1978)
13. K.B. Crozier, A. Sundaramurthy, G.S. Kino, C.F. Quate, J. Appl. Phys. **94**, 4632 (2003)
14. D.P. Fromm, A. Sundaramurthy, P.J. Schuck, G. Kino, C.F. Quate, J. Appl. Phys. **4**, 957 (2004)
15. P. Muhlschlegel, H.-J. Eisler, O.J.F. Martin, B. Hecht, D.W. Pohl, Science **308**, 1607 (2005)
16. F. Jackel, A.A. Kinkhabwala, W.E. Moerner, Chem. Phys. Lett. **446**, 339 (2007)
17. R.D. Grober, R.J. Schoelkopf, D.E. Prober, Appl. Phys. Lett. **70**, 1354 (1997)
18. K. Sendur, W. Challener, J. Microsc. **210**, 279 (2003)
19. E.X. Jin, X. Xu, J. Comput. Theor. Nanosci. **5**, 214 (2008)
20. L. Novotny, Phys. Rev. Lett. **98**, 266802 (2007)
21. A. Hartschuh, E.J. Sánchez, X.S. Xie, L. Novotny, Phys. Rev. Lett. **90**, 095503 (2003)
22. K. Sendur, W. Challener, C. Peng, J. Appl. Phys. **96**, 2743 (2004)
23. L. Wang, X. Xu, J. Microsc. **229**, 483 (2008)
24. B. Liedberg, C. Nylander, I. Lundstroem, Sens. Actuators **4**, 299 (1983)
25. Y. Ohdaira, T. Inoue, H. Hori, K. Kitahara, Opt. Express **16**, 2915 (2008)
26. K. Sendur, E. Baran, Appl. Phys. B **96**, 325 (2009)
27. E.D. Palik, *Handbook of Optical Constants of Solids* (Academic Press, San Diego, 1998)
28. L. Novotny, B. Hecht, *Principles of Nano-Optics* (Cambridge University Press, New York, 2006)
29. K.L. Kelly, E. Coronado, L.L. Zhao, G.C. Schatz, J. Phys. Chem. B **107**, 668 (2003)